

Energy Transfer Mechanism for a Synchrotron X-ray Gas Absorber

Álvaro Martín Ortega¹, Yves Dabin¹, Ana Lacoste², Tiberiu Minea³

¹European Synchrotron Radiation Facility,

²Laboratoire de Physique Subatomique et Cosmologie,

³Laboratoire de Physique des Gaz et des Plasmas.



Introduction: High-power absorbers are necessary to protect the optical elements of a beamline. Gas ones offer a stress-free medium but with variable density, due to thermal gradients and pressure variation

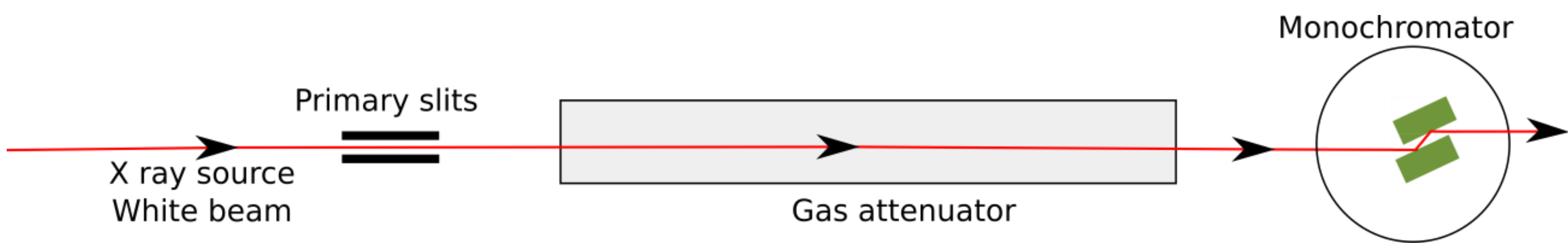


Figure 1. Schematic setup of a gas absorber.

CFD model: A 2D model was set up to study the effect of thermal convection in the heat transfer and to obtain the relation between power input and central density.

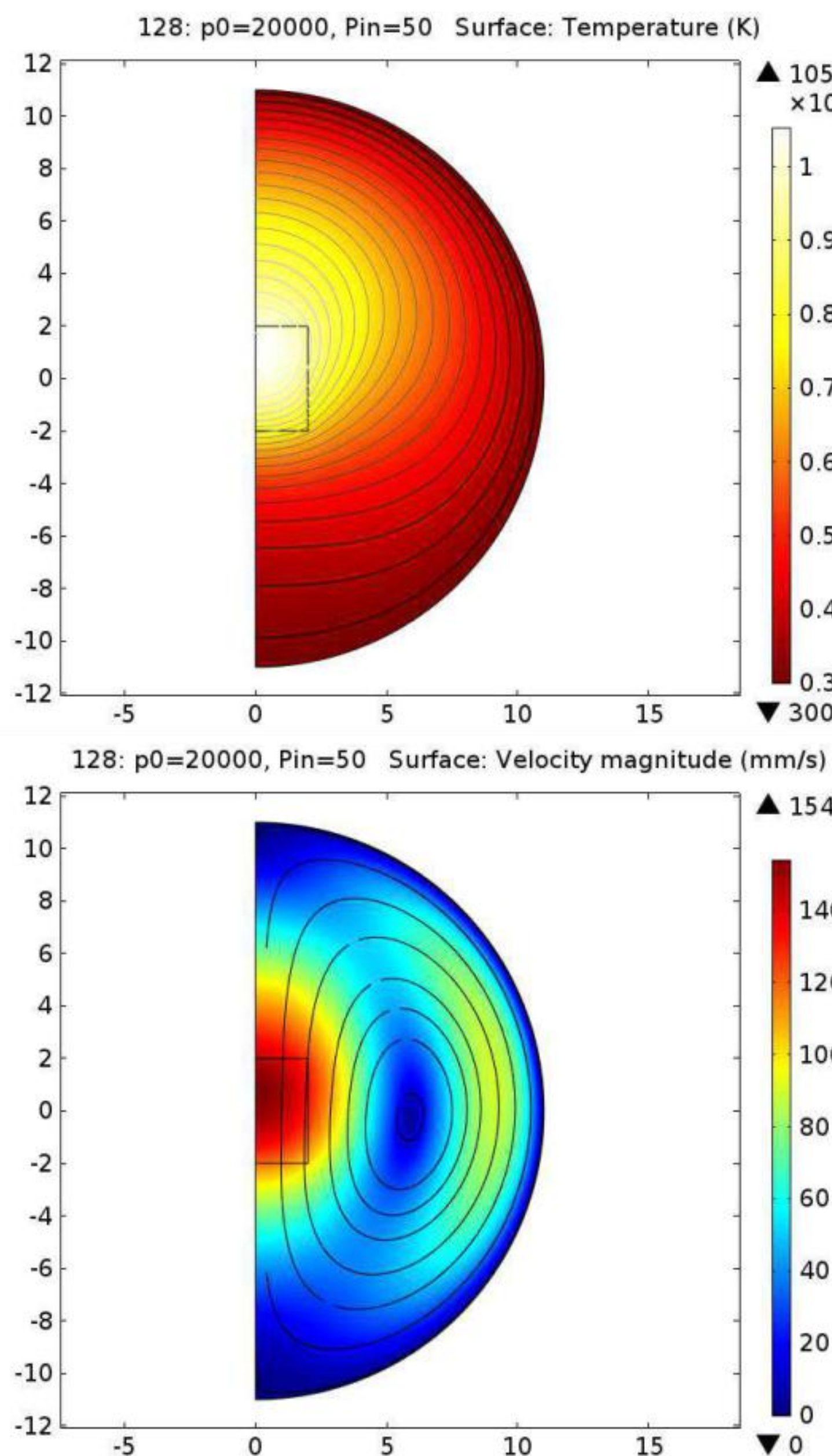


Figure 2. Temperature (top) and velocity (bottom) profiles.

There is no hot plume ascending from the heated area towards the top of the circumference, and the temperature profile is not very distorted from that of pure thermal conduction.

The Rayleigh and Nusselt numbers obtained for the pressure and power range of interest (50-500 mbar, 0-700 W) also show that the deviation from the pure conduction (Nu=1 and low Ra) is small and can be neglected in a first approximation.

$$Ra = \frac{C_p \mu}{k} \cdot \frac{g \rho_0 (T_h - T_c) L^3}{T_0 \mu_0^2}$$

$$Nu = \frac{L}{k_0 (T_h - T_c)} \cdot k \frac{\partial T}{\partial x} \Big|_{wall}$$

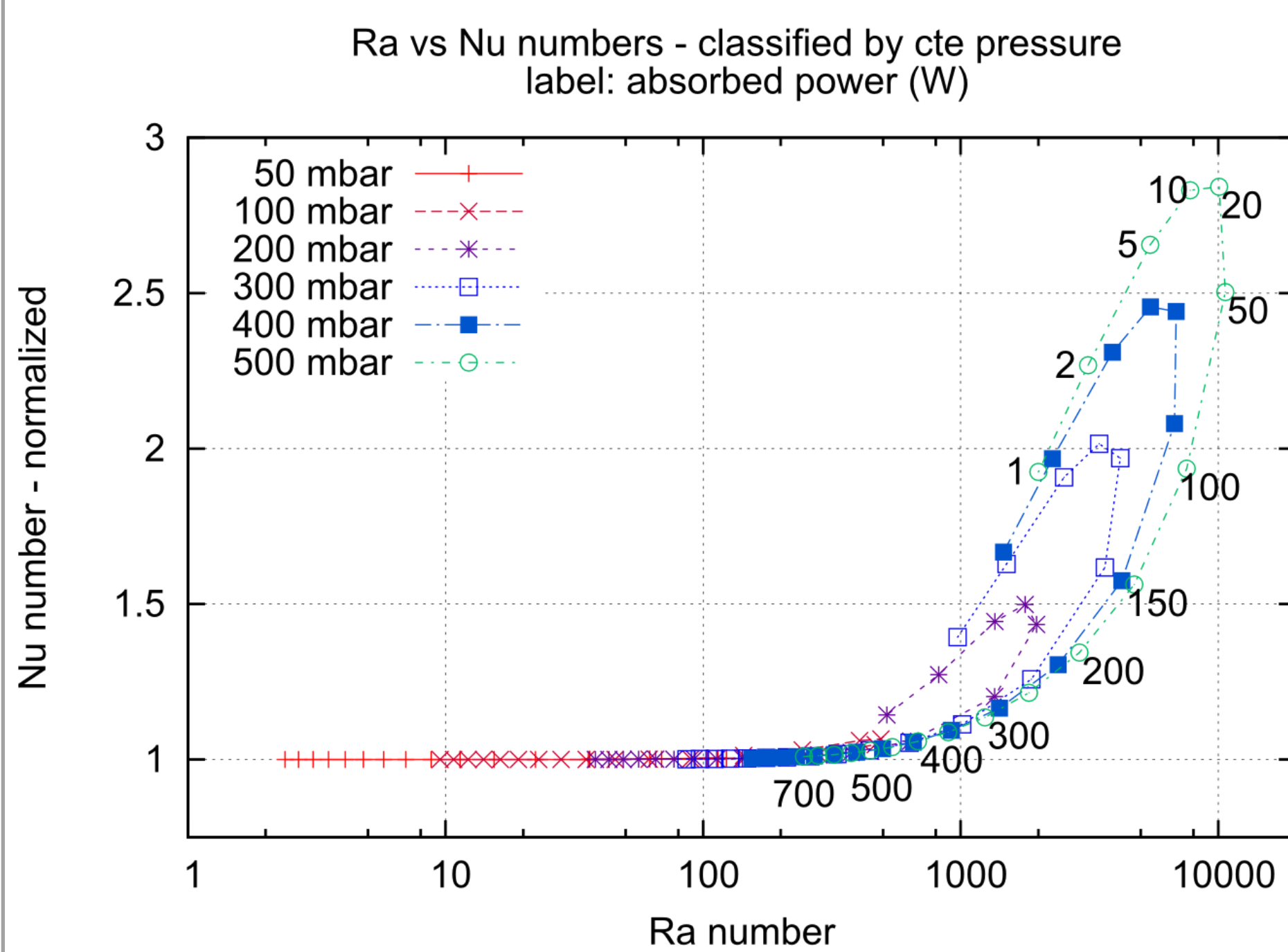


Figure 3. Ra vs Nu numbers, linked by constant pressure. The Nu number was normalized in each case with the value when only conduction took place.

Plasma model: a 1D model was set up to obtain the relation between power input and central density. This relation will be used in a pseudo-3D model taking into account the variation in the absorber power with the length.

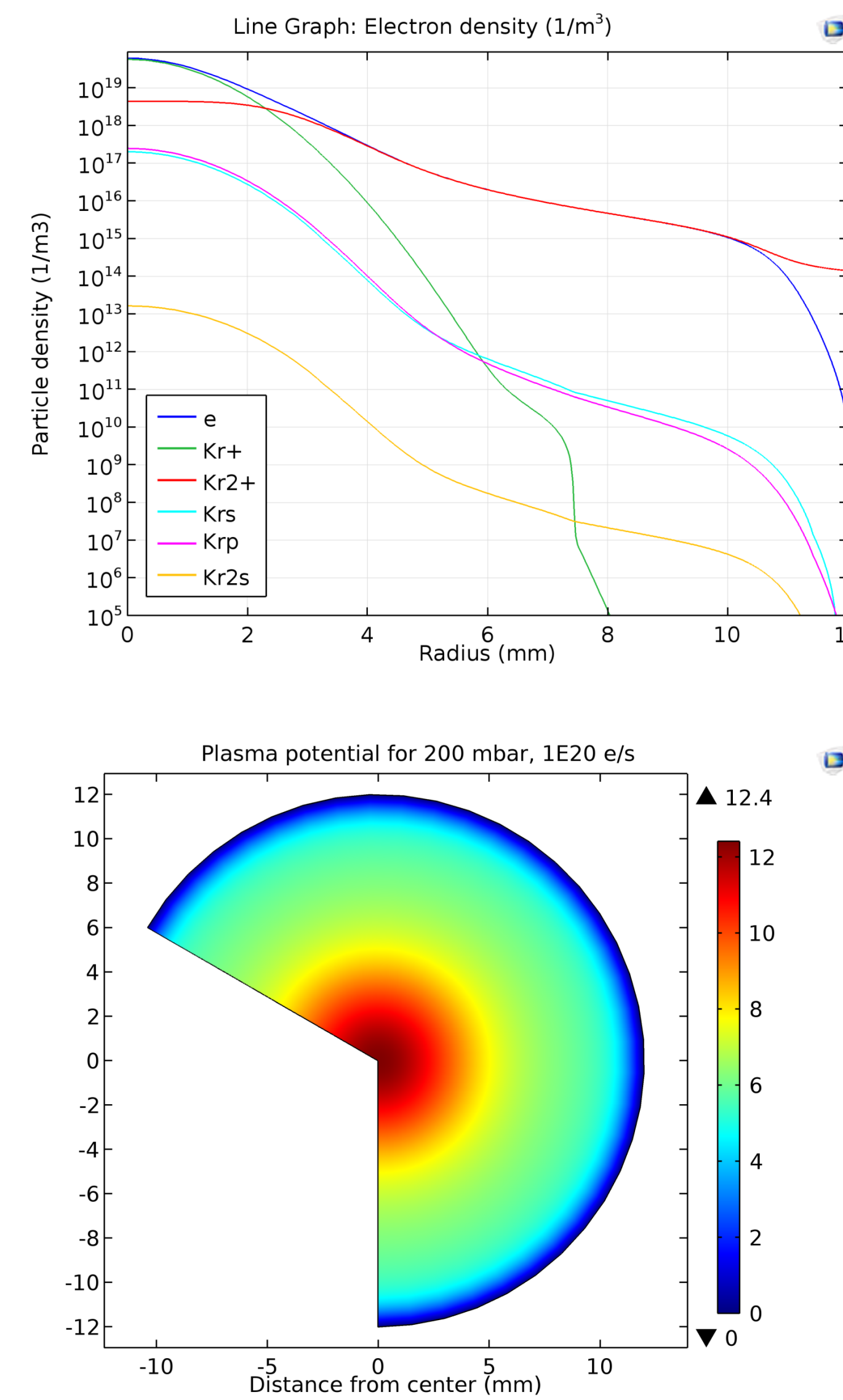


Figure 4. Particle concentration (top) and plasma potential (bottom)

The transport coefficients and electron-impact reaction rates were calculated from the cross sections using BOLSIG+ and assuming a maxwellian EEDF. The heavy species reaction rates were taken as constant or as temperature dependant when the data was available.

The source was a Gaussian centered around the axis, to represent the scattering of the X-ray beams. The walls of the attenuator were grounded and with no reemission of electron due to the small electrical field.

Comparison and conclusion: The model results were compared with the experimental data available from 2010 tests.

The 'plasma' results yielded a much closer result to the experiment than the purely thermal ones, due among other reasons to the inclusion of radiative deexcitation, which does not heat the gas.

Adjustment of the source balance between ions and excited species also improved the results, but to get a perfect match a Monte Carlo simulation of the high energy source (X-rays and fast electrons) is needed.

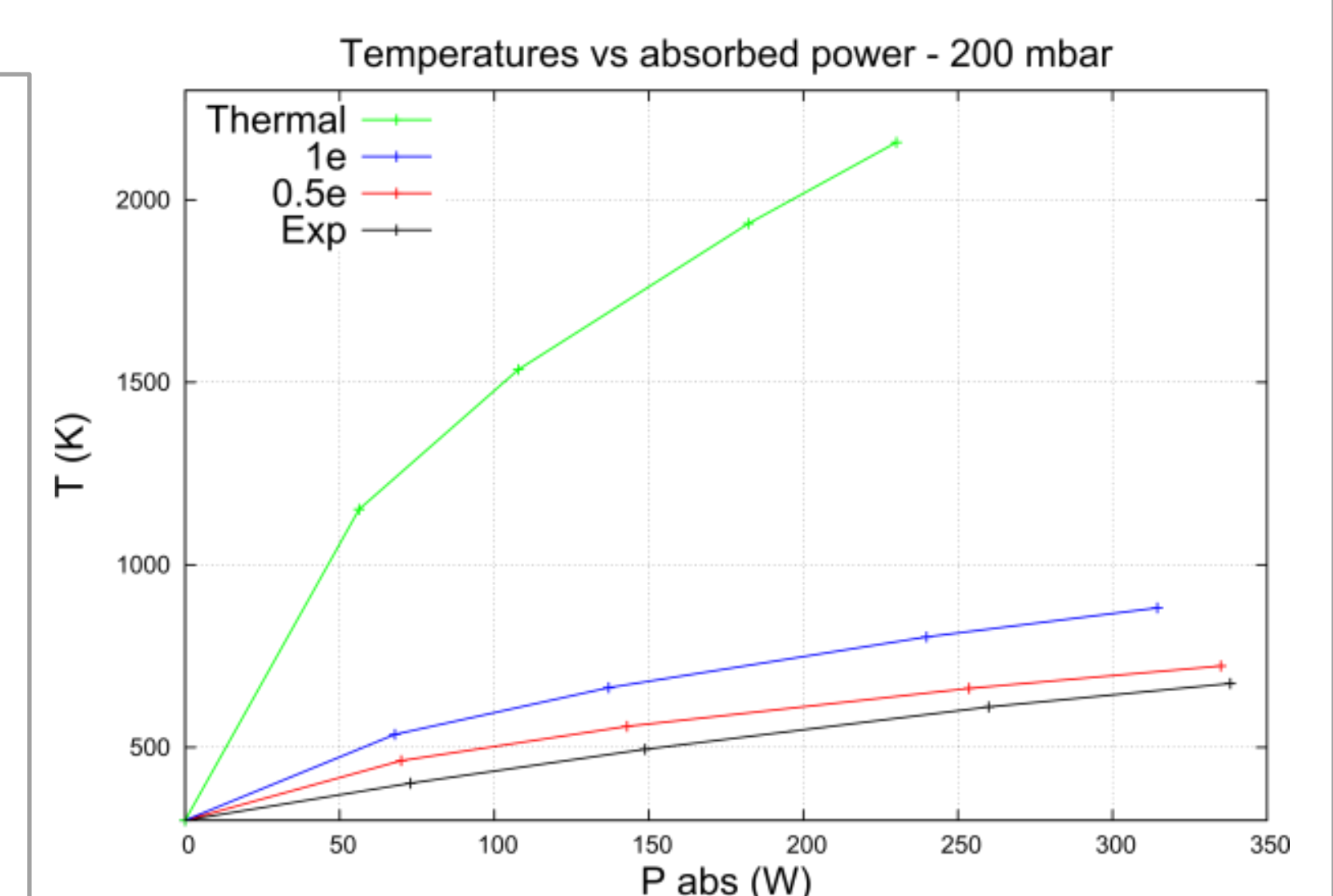
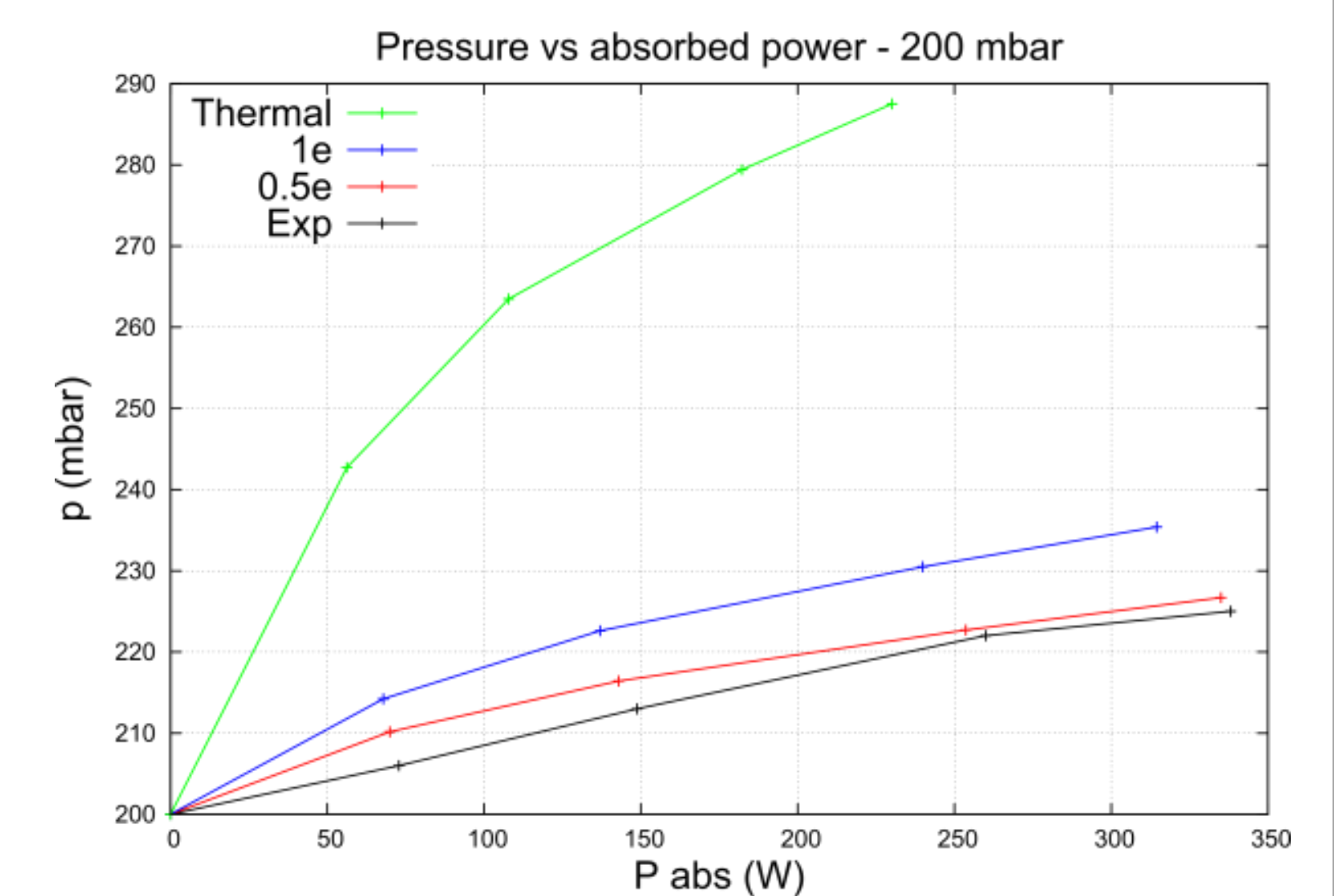
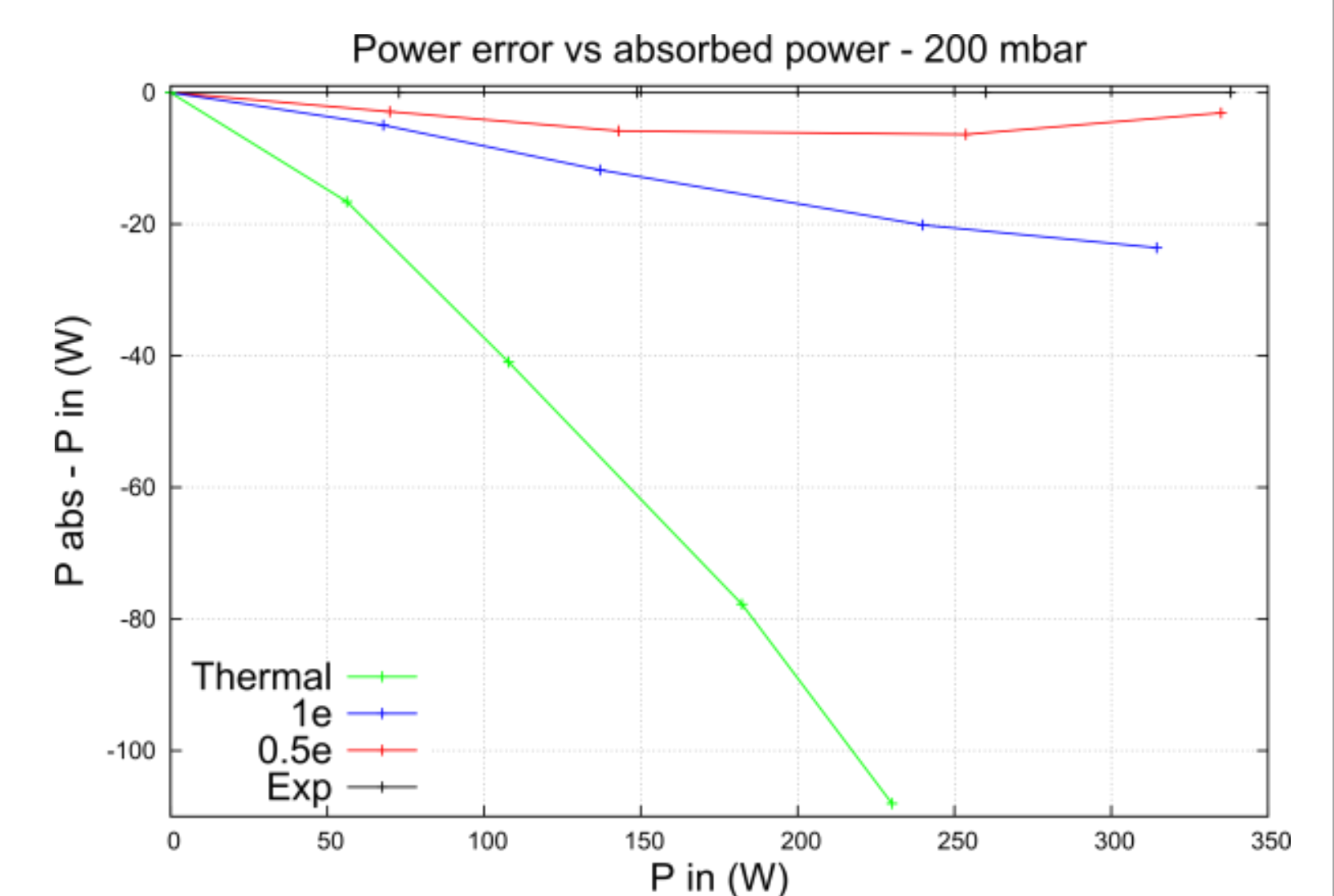


Figure 5. Experimental and model results for an initial pressure of 200 mbar and variable input power.

References.

1. Jean Susini et. al. New challenges in beamline instrumentation for the ESRF Upgrade Programme Phase II, *J. Sync. Rad.*, **21** 986-995 (2014)
2. W. Rosenhow et. al., Handbook of heat transfer fundamentals, 1985 McGraw-Hill.
3. Biagi-v8.9 database, www.lxcat.net, retrieved on June 1, 2015 / Cross sections extracted from Program Magboltz, Version 8.9 March 2010
4. P. Lukáč et. al., Dependence of the dissociative recombination of molecular ions Kr_2^+ with electrons on the electron and gas temperatures, *Plasma Sources Sci. Tech.*, **21** 065002 (2012)
5. S. Bendella et. al., Modelling of Kr-Xe discharge of sxcimer lamp, *EPJ Web of Conferences*, **44** 04004 (2013)
6. C. Flores, Study of a gas absorber for Synchrotron's light, Master Thesis, UPM (2010)